Luleå University of Technology

Polar Atmospheric Physics

F7014R

EISCAT Space Weather

Authors
A. Hoehne
D. Talavera
E.F.M. Weterings

Supervisors
A. Tjulin
C.F. Enell
V. Barabash

June 20, 2019

Table of Contents

1   Introduction

The purpose of this report is to relate space weather events with analyzed data from EISCAT. The end result of this practical is to become acquainted with data from EISCAT and the programs used to analyze it. This report will be analyzing data from the EISCAT radar through the use of GUISDAP. The pre-analyzed data comes from EISCAT through Madrigal database. With GUISDAP and Madrigal, the plots will be interpreted to find relationships with space weather.

The effect from the sun and the other extraplanetary sources on the Earth is called space weather. The influence of space weather on Earth include the aurora, disturbances in magnetosphere and ionosphere, and geomagnetic induced currents [1]. The causes of the space weather originates from the sun which includes coronal mass ejections, solar flares, and coronal holes. There are several effects originating from space weather: damaging spacecraft electronics, increased drag affecting orbit of satellites, increasing radiation dosage in astronauts and airplane passengers, causing radio blackouts on Earth, and causing electrical power grid power outages. Space weather can be observed by ground-based systems or by satellites. Ground-based systems involve telescopes observing the photosphere, neutron detectors, and measuring the ionosphere. Many current satellites carry sun monitoring sensors as secondary payloads. There are mathematical models that can simulate the space weather environment.

The space weather event studied mostly in this report occurred between October 19th and November 7th and is referred to as the Halloween solar storms. It occurred during the later part of solar cycle 23. It was not expected during the quieter part of the solar cycle. It had a large affect on Earth, with aurora seen in Florida, satellites and communications being affected, and a power outage is Sweden lasting for a hour [2]. It was composed of 17 flares ranging in strength, with the largest being estimated at X28 power causing a R5 radio blackout and numerous anomalies in satellites [3].

2 GUISDAP software

In this section the raw EISCAT data is processed using the MATLAB software with the package GUISDAP. The data analyzed in this section was obtained with the 42m radar located in Svalbard, Norway. The time frame of the analyzed data corresponds to the 27th of October, 2016, from 15:00 to 21:00.

GUISDAP have several "experiment" methods. From the EISCAT experiments manual: "An EISCAT experiment is a set of instructions telling the transmitters, receivers and digital signal processing units what to do at what time". Meaning that depending on the object of interest of the experimenter, Some of the parameters that change between experiments are the code length in bits, baud length, smapling rate, the range span (measurable height), time resolution, etc. In this particular case, the experiment "ipy" was used.

With the help of GUISDAP, a few plots showing different parameters observed in the ionosphere at the time period mentioned above. The following parameters are used by the ipy experiment. One of the obtained parameters is the raw electron data. The data obtained with GUISDAP which is data measured from the EISCAT radar, was compared with data formulated using the IRI model in the following pictures.
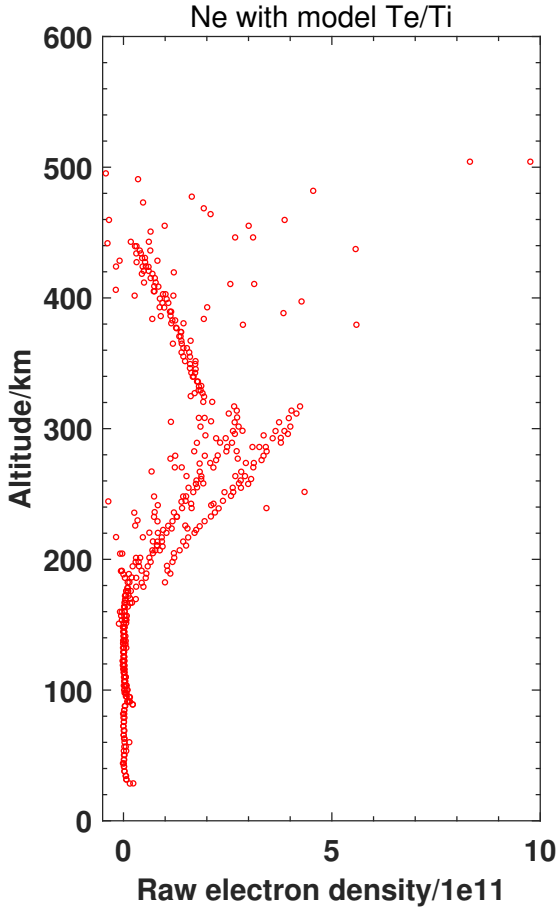

Figure 1: Electron density data obtained from EISCAT 2016-10-27.
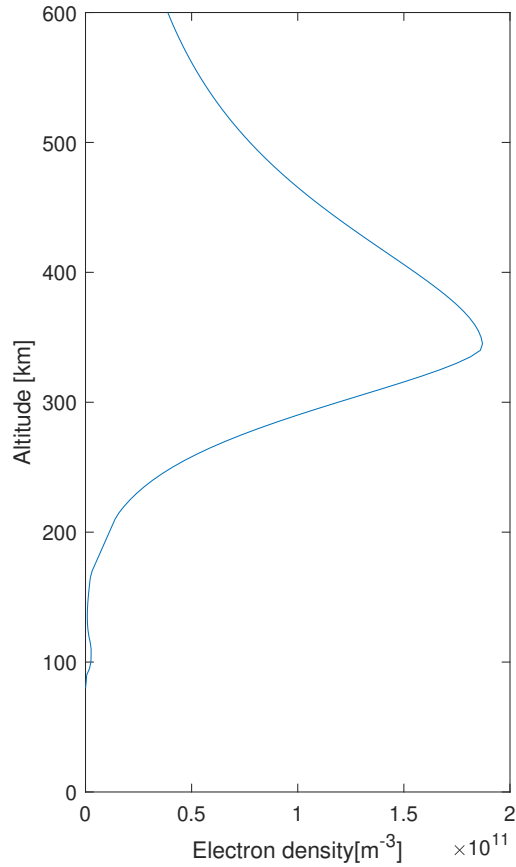
Figure 2: Electron density data from the IRI model 2016-10-27

In these two images, the electron density from 0 to 600 km was plotted in order to compare the IRI model to the measurements from EISCAT. Both are showing the electron density distribution at around 18:00 hours. While both the model and measurements agree on where the maximum occurs, the model underestimates the amount of electrons by about a factor of 3. More on the IRI model will be discussed in a later chapter.

Produced@DESKTOP-10LDCOV, 10-May-2019   Not for publication - see Rules-of-the-road
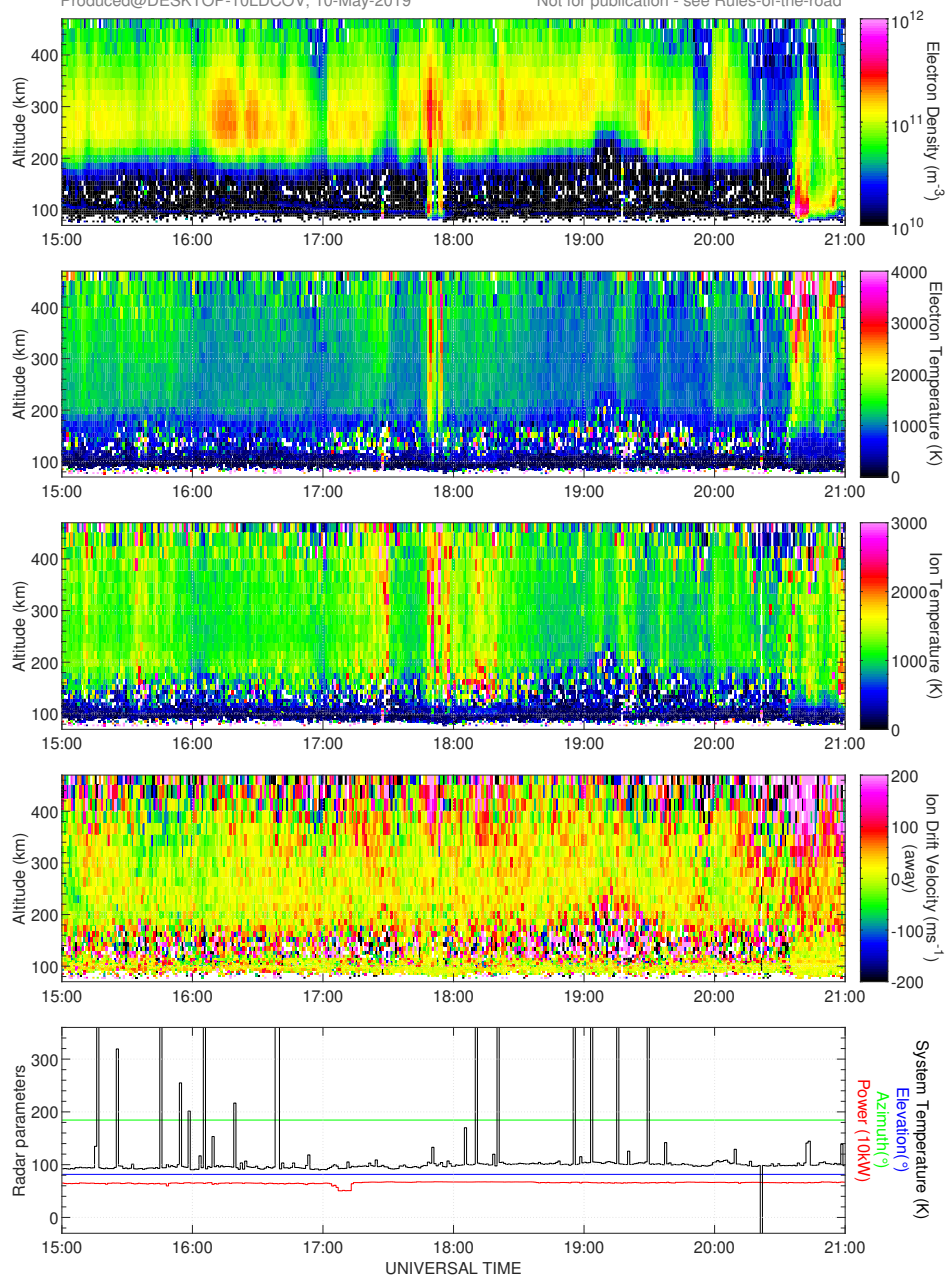

Figure 3: Plot produced analyzing raw data from EISCAT with GUISDAP

4

Figure 3 shows the results of analyzing 6 hours of data obtained by EISCAT from 15:00 to 21:00 on the 27th of October 2016. In the first row, we can see the electron density which matches with the plots on figure 1 and figure 2, showing a maximum around 300 km of altitude. The second row shows the electron temperature, with respect to each altitude, it is interesting to note that most of the times the variation is smooth and small, except for a small band right before 18:00 and a larger band around 20:30. The third row row shows the ion temperature, again, this one is more or less constant along time with a few exceptions around 17:30 and 18:00. The fourth row showing the ion drift velocity, most of the values look like a more or less random noise, meaning that this drift velocity is not consistent. On the fifth and final row we see the data of the antenna within the time range of the data analyzed.

During the time of he data analyzed, it can be seen that the electron density is higher starting from around 16:15 with a peak right before 18:00 at around 300km of altitude and then again before 21:00 at around 100km. The latter peak, along with a high electron temperature between 300 and 400km can signify that aurora was present in the night sky at the moment.

3 Space weather event

In the rest of this document preprocessed data is used from the Halloween 2003 space weather event. This event took place from the 28th up to the 29th of October, with the main two peaks at 11:10 (28-10-2003) and 20:50 (29-10-2003) [5]. This solar weather event consisted of a series of solar flares and coronal mass ejections. The solar flare with the most energy was measured at 10:16:53 UCT. With an energy of $6.9 \cdot 10^{25}$ Joule and a mass of $1.6 \cdot 10^{10}$ gram [6], one of the strongest ever measured by GOES.

Satellite-based systems and communications were affected, as well as the instruments onboard [7]. Aircraft were advised to avoid high altitudes near the polar regions, and a one-hour-long power outage occurred in Sweden as a result of the solar activity. Auroras (figure 4) were observed at latitudes as far south as Texas and the Mediterranean countries of Europe [8].
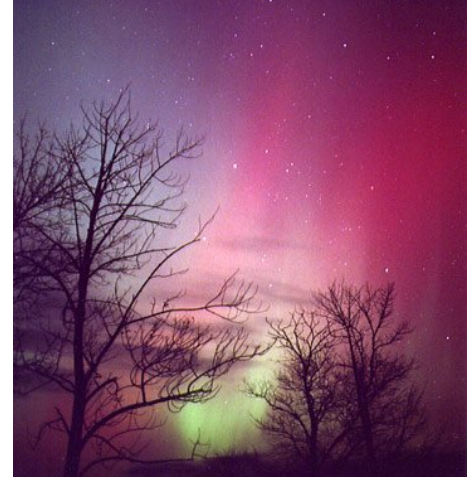

Figure 4: Geomagnetic storm/ Aurora on the 29th of October [4].

3.1 Solar flares

On the 28th 12:18 UCT one of the most powerful Coronal Mass Ejections (CME) in years erupted, this eruption, that caused a intense geomagnetic storm, is shown in figure 5.The solar flares erupted out of 486 giant sunspots. It was measured X17 on the Richter scale of solar flares. This means that the peak had an energy above $7 \cdot 10^{-4} \, \text{W/m}^2$. It was also classified as a S3 storm, which means it has a flux of more than 10^3 with $\geq 10 \, \text{MeV}$ particles. [4].

3.2 GOES

In figure 6 the space weather data from GOES10 (10th Geostationary Operational Environmental Satellite) over the month October is shown. In figure 7 the data from the same satellite is shown over the month of November [9].

In the top plot the peak flux of the solar flares/ CMEs in watts per square meter (W/m^2) between 1 and 8 Ångströms. Based on the flux the solar flare is classified. These are the classifications:

Figure 5: Solar image of a CME using a cronagraph[4].

1. Class A: flux $< 10^{-7}$

2. Class B: $10^{-7} \leq$ flux $< 0^{-6}$

3. Class C: $10^{-6} \leq$ flux $< 0^{-5}$

4. Class M: $10^{-5} \leq$ flux $< 0^{-4}$

5. Class X: flux $\geq 10^{-4}$

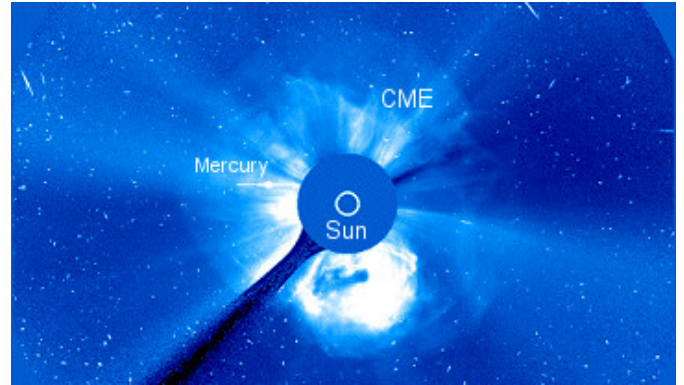In the second top plot the electrons flux, directed to Earth, is shown in $\text{e}^- \text{cm}^{-2} \text{s}^{-1} \text{sr}^{-1}$. With the black line presenting electrons with an energy greater than $0.6 \, \text{MeV}$, red above $2 \, \text{MeV}$ and green above $4 \, \text{MeV}$. In the third plot the proton flux is shown, with the energies greater than $1 \, \text{MeV}$ for black, $5 \, \text{MeV}$ for red, $10 \, \text{MeV}$ for green, $30 \, \text{MeV}$ for pink, $50 \, \text{MeV}$ for blue, $60 \, \text{MeV}$ purple and $100 \, \text{MeV}$ for light blue. In the last plot the magnetic field strength in nT, where black (Hp) is the magnetic field vector component, points northward, perpendicular to the orbit plane which for a zero degree inclination orbit is parallel to Earth's spin axis. Red (He) is the magnetic field vector component, perpendicular to Hp and Hn and points earthward. Green (Hn) is the magnetic field vector component, perpendicular to Hp and He and points eastward.
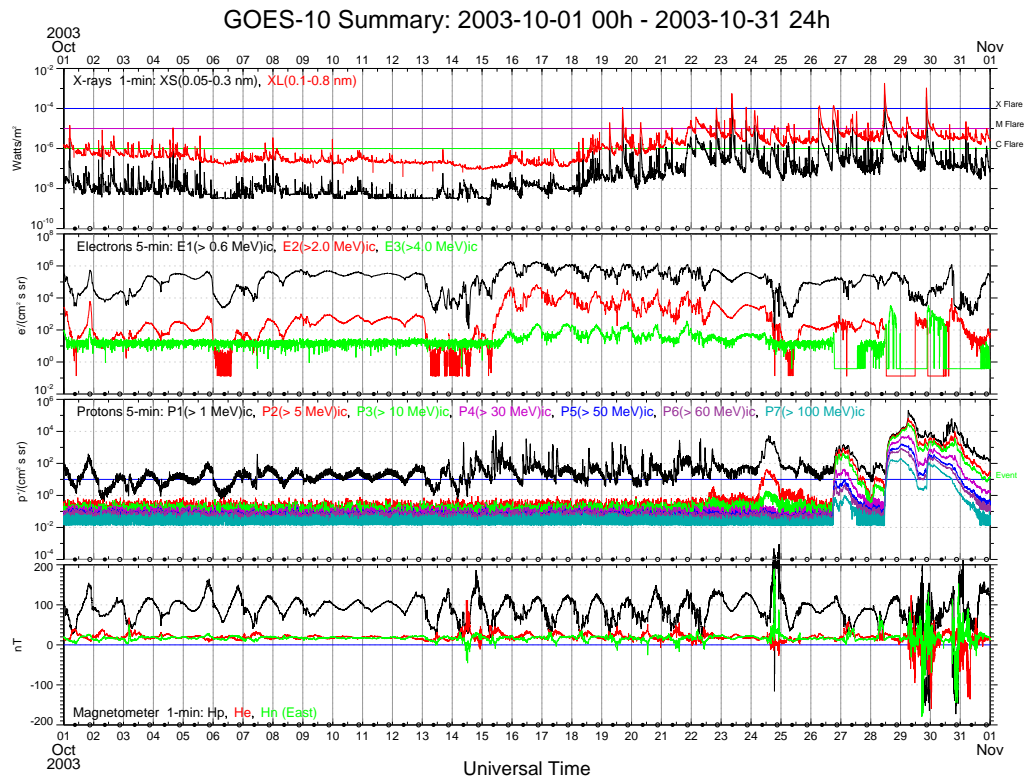
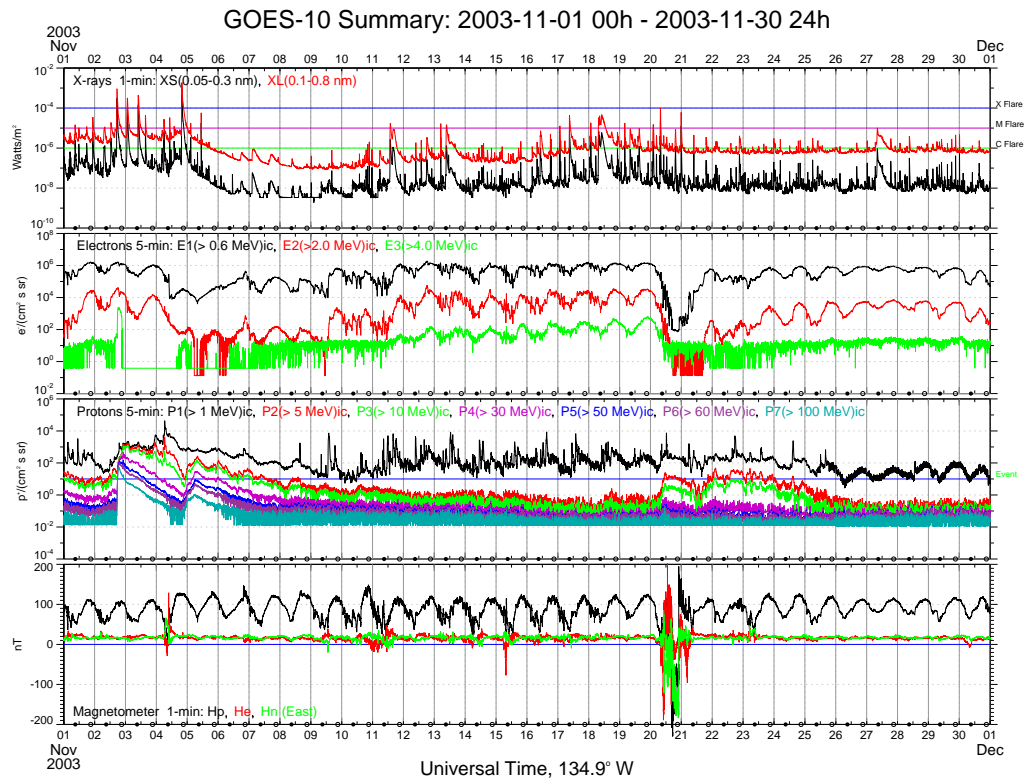Figure 6: GOES10 data from the month October 2003 [9].

Figure 7: GOES10 data from the month November 2003 [9].

From the GOES data in figure 6 and 7 it can clearly be seen that the were a lot of instabilities during the end of October and the beginning of November. Starting around the 14th of October the magnetic field became more instable and the proton flux increased. On the 18th the electron flux increased, as well as the flux of energy. The main two peaks where at the 28th and 29th of October, followed by some less, but still pretty strong, flares on the 2nd, 3rd and 4th of November. After the sixth of November the fluxes went down again.

3.3 IMAGE

In figure 8 the magnetometer data from multiple latitudes on Earth from the 29th of October to the 1st of November is shown. These values differ from the magnetometer data from GOES due to that GOES is orbiting Earth and these magnetometers are located on a fixed position on the Earth. It can be seen that the latitudes around the Auroral oval have the largest spikes.
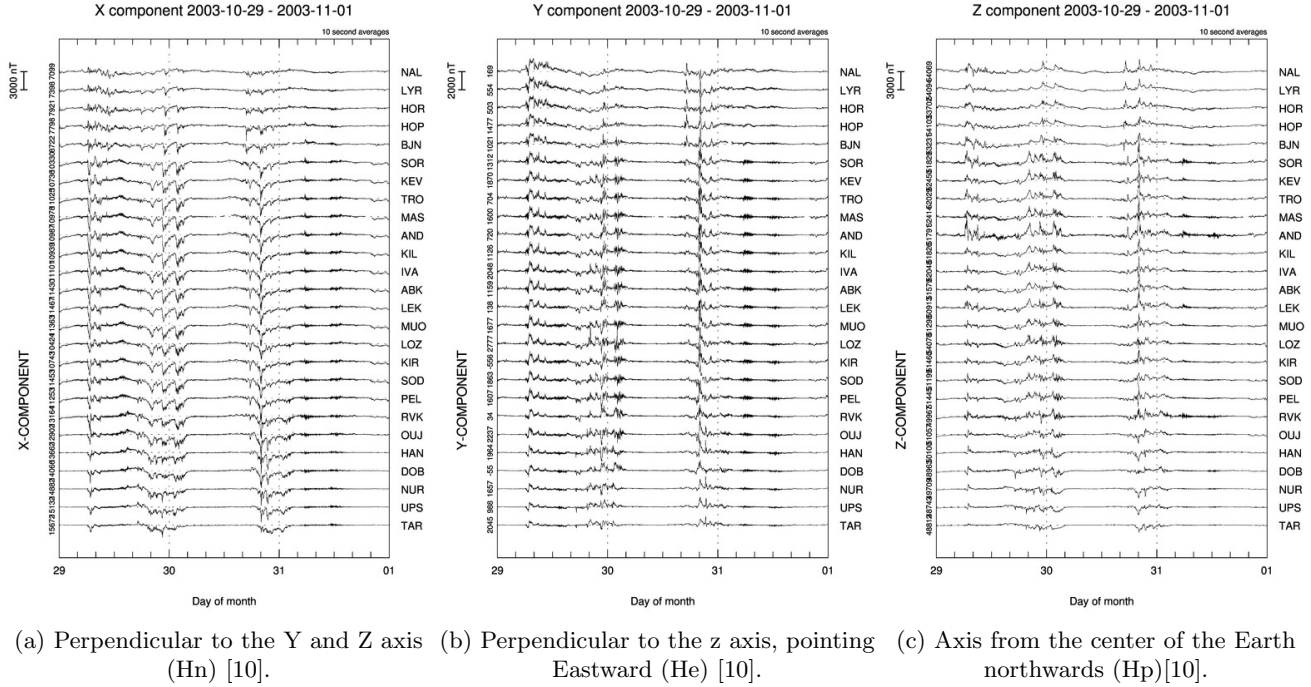

(a) Perpendicular to the Y and Z axis (Hn) [10].   (b) Perpendicular to the z axis, pointing Eastward (He) [10].   (c) Axis from the center of the Earth northwards (Hp)[10].

Figure 8: Magnetogram data from IMAGE (International Monitor for Auroral Geomagnetic Effects).

4   EISCAT Madrigal

In figure 9 the EISCAT data from the 30th of October 2003 is shown. There are a few white gaps which can be explained by interference like clouds in the atmosphere. On top we have the electron density, followed by the electron temperature, ion temperature, ion drift velocity and the system temperature.

Around 20:50 on the 29th of October 2003, one of the main peaks during this solar storm was measured. When this peak was over there was a dip in electron density, as can be seen from figure 9. Then, on the 30th of October there were some M-flares at 1:55 till 2:45 and 15:20 till 15:40 measured by GOES [5]. You can see in the EISCAT data that right after this change has been measured the densities and temperatures started increasing. The peaks are delayed by a a couple of hours in this data.

When comparing the data from the 30th of October 2003 to a more quit day, like the one in figure 3, it can be seen that especially the fluctuations are way more intense. The gradient between upper and lower in the atmosphere is still present. But everything is, on average, more intense. The perturbations go deeper into the atmosphere and with higher velocities.
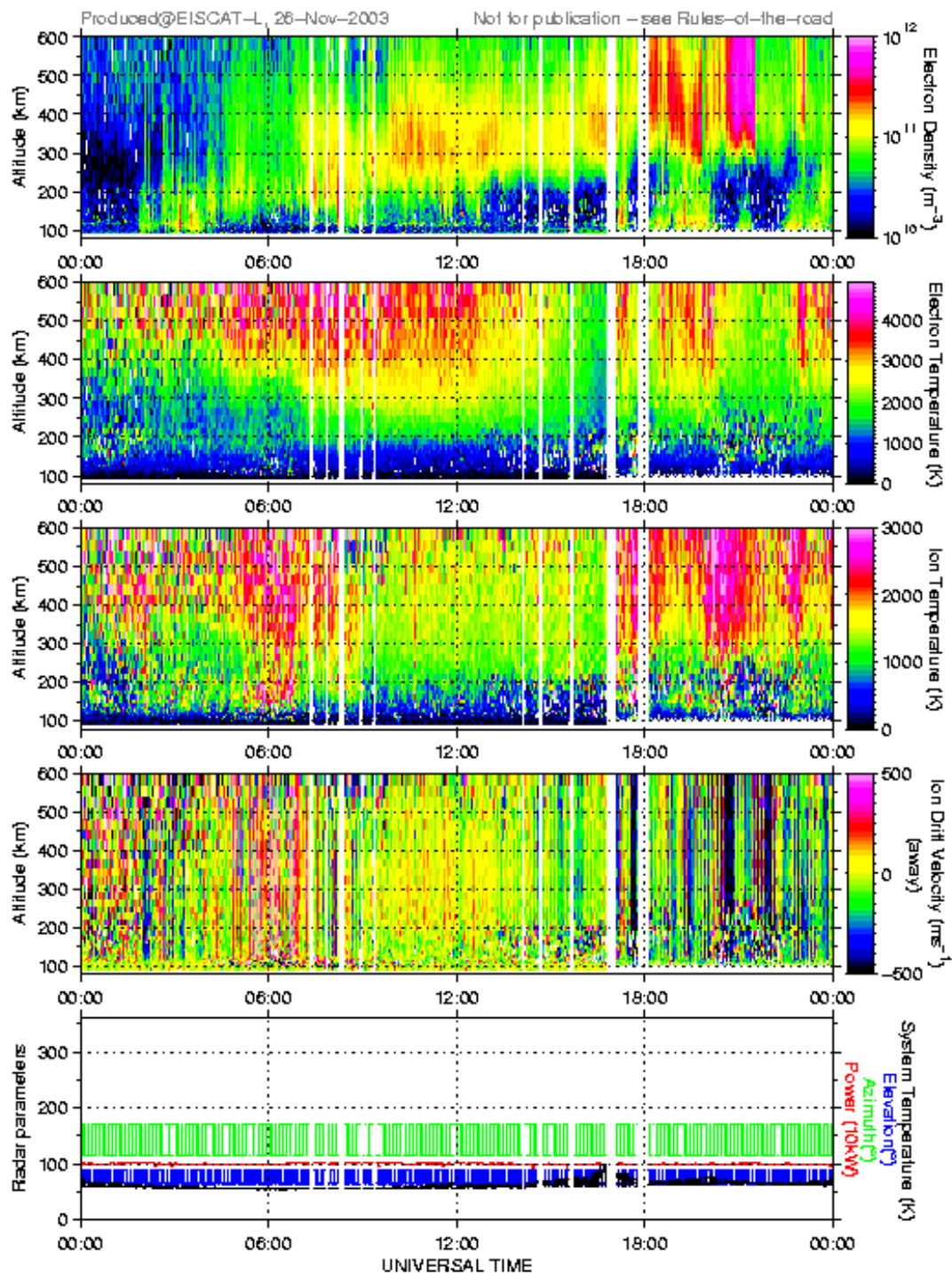
Figure 9: EISCAT radar data from the upper atmosphere science database Madrigal [11].

5 International Reference Ionosphere (IRI)

This model has been developed by an international collaboration sponsored by the Committee on Space Research (COSPAR) and the international Union of Radio Science (URSE). The development started in the late sixties in order to create a standardized model of the ionosphere by compiling empirical data from the available sources at the time. this model has been updated several times in order to keep it up to date with current measurements. The data of IRI comes ionosondes, incoherent scatter radars, satellites and sounding rockets.

A comparison was made between the data from the IRI model and the data obtained with EISCAT's incoherent scatter radar in Svalbard, Norway. This comparison takes data at around 21:01 hours on the 30th of October of 2003, as part of the Halloween solar storms.
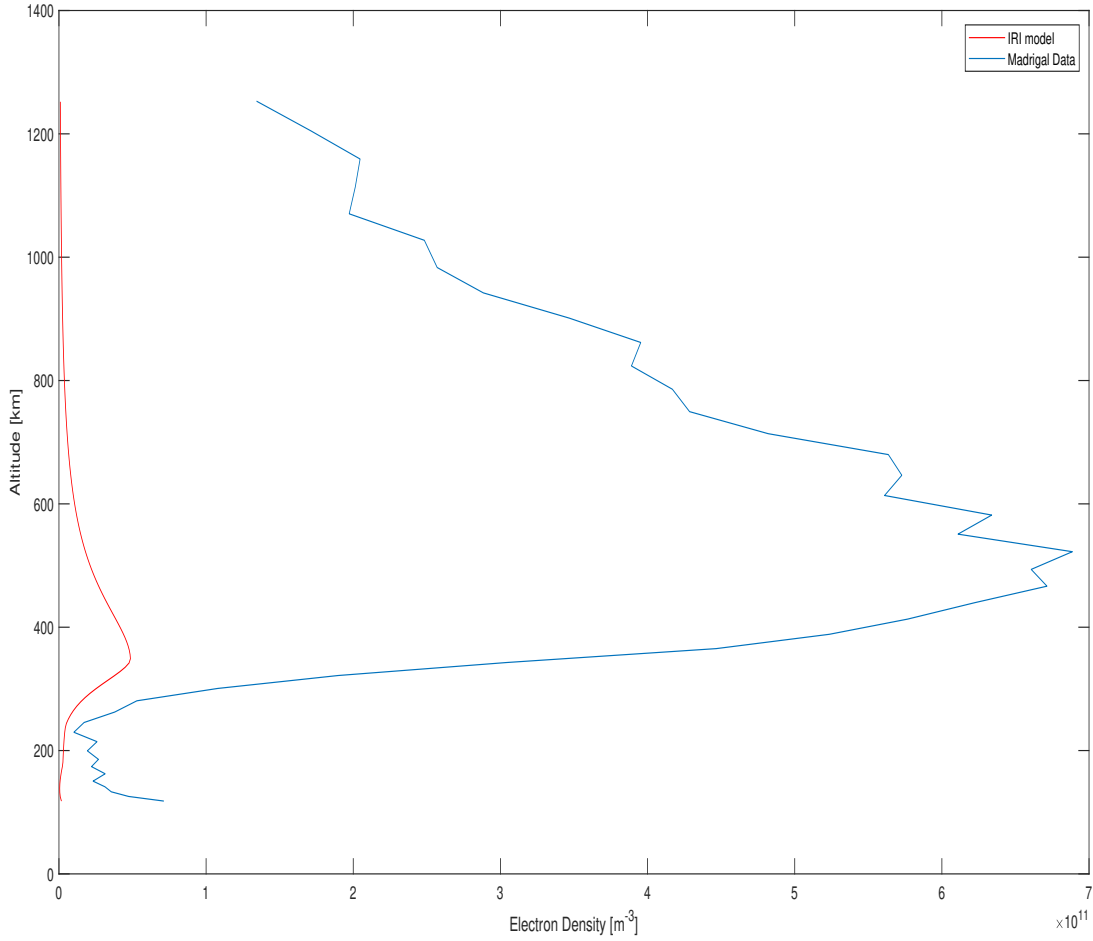

Figure 10: Comparison of the IRI model data (red) and the one obtained from EISCAT through the Madrigal system (blue).

While both sources more or less agree where the maximum of electron density occurs. There is a big discrepancy in the values shown, of about one order of magnitude.This can be attributed to the fact that the IRI model uses a monthly average to display the electron density of a particular time and date.

6 Discussion

The effects of solar flares are easily observed in Figure 9. There is a strong increase in the electron density, a decrease in electron temperature, fluctuations in the ion temperatures, and changes in ion drift values. Handzo [12] looked at X-class flares effects in the atmosphere and saw strongly increased electron density peaking after the the flare and the perturbation lasting a long time. This large difference between the actual electron density and the IRI-model estimate is shown in Figure 10. The electron density during the storm is approximately a magnitude larger than the approximated model. The disturbance peaked after the solar flare and lasted for approximately an hour afterwards. After this time period, the electron density suddenly enters a depleted state with a lower electron density than prior to the flare. The electron temperature is shown as decreased during and after the solar flare. This is contrary to the accepted notion of highest electron temperatures during the strongest solar storms [13]. This discrepancy between the the data shown and the expected results of the higher temperatures could be explained with differentiated plasma. This concept is explained in Battaglia [14], where there is cool core and the heated outer regions. Battaglia mentioned this could also be due to the cooler plasma in the foreground interacting with the higher temperature plasma. During a solar flare, the ion temperatures can fluctuate during the solar storm due to positive and negative effects [15]. The ion temperature and the ion density interact interact causing an unpredictable variations. The temperature for the case of this Halloween storm fluctuated but remained higher than normal. The solar flare has a positive and negative effect on $E \times B$ ion drift velocities [16]. There is a short lasting severe decrease in velocities and a longer lasting, much weaker increase in ion velocities.

7 Conclusion

This report looked at the effects of the solar flares from Halloween 2003 on the ionosphere. As well as into the data provided by EISCAT and Madrigad, to draw conclusions about the effects of solar flares on ionosphere. The effects of the flare were very typical and was expected. The effects of the solar flare were clearly presented in the figures shown in the report. The unexpected consequence of the flare was a lower ion temperature, this was possibly due to the interactions of colder plasma in the foreground. The effects of the storm was consequential but not severe in terms of health or technology impacts. This storm should serve as warning as the potential of a larger solar flare that could irreparably damage unprotected power grids or satellites. Damages to these systems could move human progress back decades.

8 Confirmation of Participation

Hereby, A. Hoehne, D. Talavera and E.F.M. Weterings declare to have participated and collaborated in this report.

References

[1] *Space weather phenomena*, Accessed: 2019/05/07. [Online]. Available: `https://www.swpc.noaa.gov/phenomena`.

[2] B. Dunbar, *Halloween storms of 2003 still the scariest*, Accessed: 2019/05/07, May 2015. [Online]. Available: `https://www.nasa.gov/topics/solarsystem/features/halloween_storms.html`.

[3] C. Balch, D. Biesecker, L. Combs, M. Crown, K. Doggett, J. Knuches, H. Singer, and D. Zezula, "Halloween space weather of 2003", NOAA, 2004, Technical Memorandum OAR SEC-88.

[4] T. Phillips. (2003). What's up in space, [Online]. Available: `http://spaceweather.com/` (visited on 05/05/2019).

[5] A. Möller. (2003). Goes x-ray flux archive. SWPC, Ed., [Online]. Available: `https://www.polarlicht-vorhersage.de/goes-archive` (visited on 05/05/2019).

[6] S. Yashiro and N. Gopalswamy. (2018). Soho lasco cme catalog, [Online]. Available: `https://cdaw.gsfc.nasa.gov/CME_list/` (visited on 05/05/2019).

[7] NOAA. (2003). Current space weather conditions. SWPC, Ed., [Online]. Available: `https://www.swpc.noaa.gov/products/ace-real-time-solar-wind` (visited on 05/05/2019).

[8] Wikipedia. (2003). Halloween solar storms, [Online]. Available: `https://en.wikipedia.org/wiki/Halloween_solar_storms,_2003` (visited on 05/05/2019).

[9] NOAA. (2003). Goes sem data archive. NGDC, Ed., [Online]. Available: `https://www.ngdc.noaa.gov/stp/satellite/goes/dataaccess.html` (visited on 05/05/2019).

[10] IMAGE. (2018). Image user defined magnetograms, [Online]. Available: `http://space.fmi.fi/image/www/index.php?page=user_defined` (visited on 05/05/2019).

[11] Millstone Hill, Arecibo, EISCAT, SRI International, Cornell University, Jicamarca, the Institute of Geodesy and Geophysics and the archival CEDAR site. (2019). Welcome to the madrigal database at eiscat, [Online]. Available: `https://www.eiscat.se/madrigal/` (visited on 05/10/2019).

[12] R. Handzo, J. M. Forbes, and B. Reinisch, "Ionospheric electron density response to solar flares as viewed by digisondes", *Space Weather*, vol. 12, no. 4, pp. 205–216, 2014. DOI: `10.1002/2013sw001020`.

[13] A. Caspi, S. Krucker, and R. P. Lin, "Statistical properties of super-hot solar flares", *The Astrophysical Journal*, vol. 781, no. 1, p. 43, 2014. DOI: `10.1088/0004-637x/781/1/43`.

[14] M. Battaglia, G. Motorina, and E. P. Kontar, "Multithermal representation of the kappa-distribution of solar flare electrons and application to simultaneous x-ray and euv observations", *The Astrophysical Journal*, vol. 815, no. 1, p. 73, 2015. DOI: `10.1088/0004-637x/815/1/73`.

[15] A. Bardhan, D. K. Sharma, and S. Kumar, "Variability of ion density due to solar flares as measured by sross–c2 satellite", *Indian Journal of Radio & Space Physics*, vol. 44, pp. 88–95, Jun. 2015. DOI: `10.1016/j.asr.2011.02.007`.

[16] L. Qian, A. G. Burns, S. C. Solomon, and P. C. Chamberlin, "Solar flare impacts on ionospheric electrodyamics", *Geophysical Research Letters*, vol. 39, no. 6, 2012. DOI: `10.1029/2012gl051102`.